atmosphere

MDPI

Article

WWLLN Hot and Cold-Spots of Lightning Activity and Their Relation to Climate in an Extended Central America Region 2012–2020

Jorge A. Amador * and Dayanna Arce-Fernández

Center for Geophysical Research and School of Physics, University of Costa Rica, San José 11501, Costa Rica; dayanna.arcefernandez@ucr.ac.cr

* Correspondence: jorge.amador@ucr.ac.cr; Tel.: +506-2511-5096

Abstract: Lightning activity has been recognized to have, historically, social and environmental consequences around the globe. This work analyzes the space-time distribution of lightning-densities (D) in an extended Central America region (ECA). World Wide Lightning Location Network data was analyzed to link D with dominant climate patterns over the ECA for 2012–2020. D associated with cold surges entering the tropics dominate during boreal winter. The highest D (hot-spots) was found to agree well with previously known sites, such as the "Catatumbo" in Venezuela; however, D was lower here due to different detection efficiencies. Previously reported hot-spots showed strong continental signals in CA; however, in this work, they were over the oceans near to coastlines, especially in the eastern tropical Pacific (ETP). Most cold-spots, implying a minimum of vulnerability to human impacts and to some industries, were situated in the Caribbean Sea side of Central America. The Mid-Summer-Drought and the Caribbean-Low-Level-Jet (CLLJ) markedly reduced the D during July-August. The CLLJ in the central CS and across the Yucatan and the southern Gulf of Mexico acts as a lid inhibiting convection due to its strong vertical shear during the boreal summer. The CLLJ vertical wind-shear and its extension to the Gulf of Papagayo also diminished convection and considerably decreased the D over a region extending westward into the ETP for at least 400–450 km. A simple physical mechanism to account for the coupling between the CLLJ, the MSD, and lightning activity is proposed for the latter region.

Keywords: Central America; lightning; WWLLN; hot and cold spots; CLLJ; climate

Citation: Amador, J.A.; Arce-Fernández, D. WWLLN Hot and Cold-Spots of Lightning Activity and Their Relation to Climate in an Extended Central America Region 2012–2020. *Atmosphere* **2022**, *13*, 76. https://doi.org/10.3390/atmos13010076

Academic Editor: Tomeu Rigo

Received: 5 November 2021
Accepted: 29 December 2021
Published: 1 January 2022

1. Introduction

The importance of ambient conditions for biocultural activities is well recognized by society as a way to protect lives and improve welfare. All indigenous cultures of Mesoamerica had, and still have, strong connections with sacred nature, fearing and using its signals as part of their lives. In their cosmological vision, different manifestations of the power of nature were represented by gods or goddesses [1]. In the Mayan culture (northern Central America and southern Mexico), Chaac was the God of Rain, Lightning, and Storms, all in one deity. In the Bribri-Cabécar culture (Talamanca Mountains in Costa Rica), Talayékela represented the God of Lightning [2]. These ancient cultures, most probably, considered lightning events as manifestations of the underworld in their cosmological view. Up to our times, fear of these atmospheric phenomena still prevails; however, current knowledge permits the scientific community to monitor and study these observable representations of unstable atmospheric conditions in order to mitigate their impacts on humans and industries.

Lightning activity has been recognized to have, historically, social and environmental consequences around the globe. This electrical weather phenomenon is the cause of many deaths and injuries worldwide. Approximately 2400 human casualties and 240,000 injuries occur globally every year [3]. These authors also revealed that in Mexico, the spatial

distribution of deaths is connected to exposure to thunderstorms, agricultural activities and to low-educational levels. According to the United States of America (USA) Natural Hazard Statistics (https://www.weather.gov/hazstat/, accessed on 12 May 2021), lightning is amongst the major weather killers in the USA with an annual average of 39 deaths for the period 1991–2020. That number is slightly greater than those killed by other weather events such as winter and cold surges and, it is just below the average (46) killed directly by hurricanes in that country. A recent work reports that lightning is an even major threat in the USA, being responsible for about 100 deaths per year, mainly in coastal zones [4]. In Central America alone, a total of 49 casualties and 68 injuries were reported by regional weather services during the period 2018–2019 [5–7]. As it is known, lightning strokes are forest fire starters, and they have also been shown to strongly influence pollutant levels [8]. Lightning flashes also produce disturbances in power and communication systems [9]. Recent work has stressed the value of the seasonal variability of lighting distribution in Chile, reporting that a maximum of thunderstorm days was found precisely in regions of extensive mining and where major electrical facilities for this country are built [10]. Shock waves generated by thunders in strong convective systems can often produce powerful emotions in people and collateral diseases such as Thunderstorms Asthma [11]. Electrical discharges in northern Venezuela occasionally impact human and animal zlives (e.g., cattle) and frequently affect economic activities like oil and natural gas exploitation [12]. This work reports that this activity is common in that region and that it has been named "Catatumbo Lightning" (plural), after the river of the same name.

Lightning is an intense transient electrical current that occurs in the atmosphere, mostly in a convective cloud environment. Electrical discharges may include electric currents from cloud-to-cloud, cloud to air, and cloud to the ground; however, the most frequent electrical atmospheric activity around the globe is intra-cloud release and transmission of energy. Lightning, as a chaotic system, can have different manifestations in regard to travel distances, polarity, and even in its start with a bidirectional initiation [13]. All these features, besides the lightning direction of movement and the number of branches, among others, allow various types of lightning to be identified. A complete guide to these types of lightning can be found on the Royal Meteorological Society website (https://www.rmets.org/metmatters/types-lightning, accessed on 12 May 2021).

Lightning is commonly caused by charged thunderclouds with an arrangement of positive charges above and negative charges below, like in a positive dipole configuration. The dipole structure depends on the convective activity and on the magnitude of the vertical and horizontal winds [14]. The greatest density of electrical discharges was associated with very-low cloud top temperatures in Hurricane Otto in 2016, as indicated by recent work [15]. Lightning produces whistlers, a type of very low-frequency (1 kHz to 30 kHz) electromagnetic waves that travel along the Earth's atmosphere. The ionosphere is partially permeable to these waves, and a radio atmospheric signal or "spheric" energy associated with the waves may pass through this layer all the way to the magnetosphere [16].

In this work, World Wide Lightning Location Network (WWLLN) data are used to study the spatial and temporal characteristics of lightning discharges over a prolonged extended Central America region. This territory includes parts of southwestern Mexico, the Caribbean, and a small region of northwestern South America (from here on, this region is referred to as Extended Central America (ECA). Figure 1 (inserted top left panel displays the ECA region. The spatial and temporal lightning densities (LD) were calculated, analyzed, and linked with dominant climate patterns over the ECA region. One of the aims of this paper is to identify the areas of maximum-minimum lightning densities within the ECA that have not been directly reported before in the scientific literature. Another objective of this research is to point out the regions where the lightning density is relatively low, implying a minimum of vulnerability to lightning impacts, since they represent one of the most dangerous causes of faults in the transmission lines due to electromagnetic transients [17,18], and risk the operation of electrical and electronic devices [19], and to some extent can help to diminish the investments of lightning protection systems [20].

Over the oceans, these regions can be used to compare high-low densities, as mentioned by [21] with the "coupling between large-and small-scale atmospheric electrical phenomena and various biological processes in terrestrial environments that even appear to be tied to continental waters".

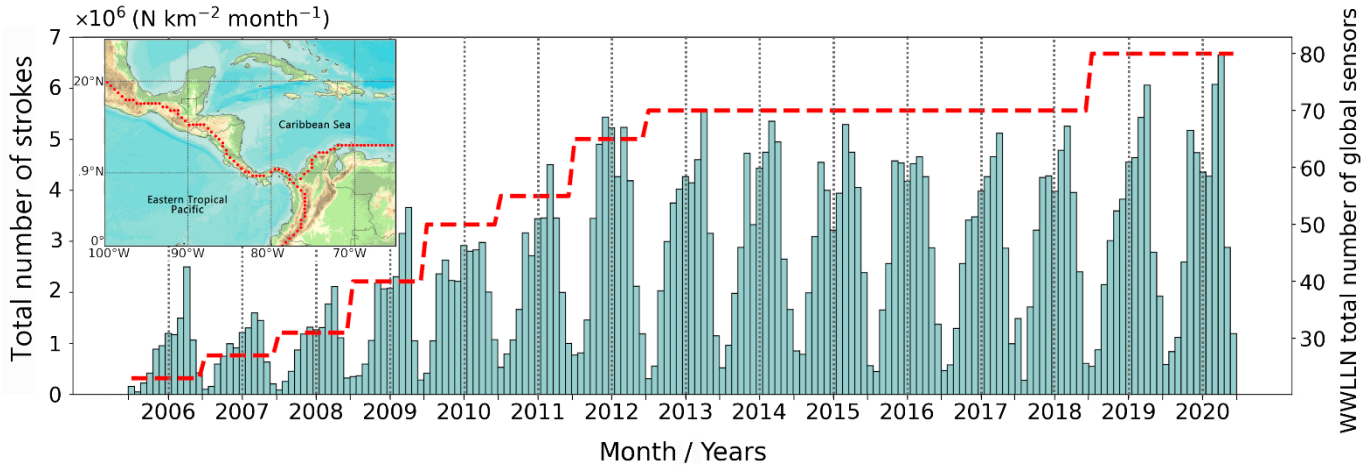

Figure 1. Total number N of strokes km^{-2} month^{-1} over the Extended Central America (ECA) region (inserted panel), and the total number of World Wide Lightning Location Network (WWLLN) sensors for each year of 2006–2020. The red broken line is the WWLLN global average number of sensors per year, approximately. The dotted red line separates, using the mountain peaks of ECA, the Caribbean, the eastern tropical Pacific basins from the northern part of South America.

To accomplish the above purpose, the ECA features selected, were the Caribbean Low-Level Jet (CLLJ) [22,23], the Choco Jet (CJ) over the Pacific slope of Colombia [24], and the Mid-Summer Drought (MSD), a reduction in precipitation during July–August over parts of Mexico and Central America [25]. The variability of the two former systems is crucial for moisture transport and regional distribution of rainfall [26–28], so they may be directly connected (or not) to convection and lightning strokes. Other convective systems, such as the Intertropical Convergence Zone (ITCZ), and cold fronts from mid and high-latitudes, were also considered in the analysis of the location of prominent electrical discharge densities. In this research, WWLLN data were also indirectly evaluated using results from other sources that reported lightning in the scientific literature, such as the activity associated with the "Relámpago del Catatumbo" [12,29], and the cloud to ground lightning distribution over Mexico [30].

This paper has been organized as follows. Some of the dominant climate attributes of the ECA are reviewed in the next section to study their potential association with the WWLLN observed time and space lightning signatures. Section 3 presents a brief account of the WWLLN progress in global data coverage since its conception in 2004–2005, circa. The WWLLN data used here are described afterward, along with the details on the methods and analysis carried out, including a discussion of WWLLN detection efficiency for the ECA. A section on results with a later discussion on their interpretation in terms of the climate systems in the region is presented, just before reaching the section on conclusions of this research.

2. Climate of the Extended Central America Region

The ECA is a region spanning from 0° N to 25° N, and from 100° W to 65° W, approximately (see the inserted panel in Figure 1). The ECA is home to a great variety of weather and climate systems characterized by broad ranges of space and time scales. Among these, the ITCZ, a relatively narrow region with strong convection [31–33], the MSD [25]; the CLLJ [22,23,34,35], and the ECA warm pools [36,37]. Tropical cyclone seasonal distribution [34,35], and the cold southward surges reaching the tropical region [38–41], are

systems with the vast convective potential to turn on and off the lightning activity in this region. Some of the prominent geographical features of the ECA that can potentially drive convection are described in [23,34,35].

The ITCZ presents a broad band of convection modulated by the moisture convergence flux driven by the trades coming from both sides of the Equator. This climatic component shows a meridional migration in phase with the mean sun relative position in the Northern Hemisphere [32,42]. Following [25], precipitation over southwestern Mexico and the Pacific slope of Central America is described by a bimodal distribution; the maxima of precipitation occurring during June and September–October with a minimum of convective activity and precipitation (MSD), during July–August. In contrast, over the western Caribbean side, a minimum of precipitation is observed during April and October, with a maximum during July–August in its southwestern part (approximately). A secondary rainfall peak is also detected in the latter region associated with the intrusion of cold fronts during the winter months [38–41,43].

A dominant climate feature of the ECA is a strong easterly low-level wind current that extends from the easternmost part of the Caribbean Sea (CS) to the eastern tropical Pacific (ETP) [23]. The MSD over Mexico and Central America has been associated with the intensity and role of the CLLJ [23,44]. Changes in wind strength are associated with the annual precipitation distribution over Central America. When the MSD takes place along the Pacific coast showing stronger than normal winds during a warm El Niño Southern Oscillation phase, the Caribbean slope shows a maximum of precipitation [23,25]. The CLLJ also presents a notable region of strong moisture flux convergence (divergence) that is associated with the exit (entrance) of the jet at low-levels [22,23]. The former territory is near Central America between Costa Rica and Nicaragua, and the latter is in the central CS. The CLLJ shows wind maxima in July and January-February near 925 hPa with values in excess of 13 m/s [23,34,35]. In the above two seasons, the CLLJ presents regions of low-level converge-divergence (discussed above), except that the former is more intense than the latter. This current presents relatively weak intensity (4–5 m/s) during September–October to early November. As a consequence of this seasonal decrease in the CLLJ low-level strength, the vertical wind shear is reduced over the CS, hurricane activity peaks [34,35,45], and rainfall spreads regionally as a result of tropical cyclone activity, the ITCZ northward migration and traveling easterly waves, among other systems. During late November and early December, the trades increase again, and the CLLJ winter component reaches the other intensity peak. The CLLJ transports large amounts of humidity from the CS to Central America, to southeastern Mexico and across the Gulf of Mexico to the southern USA [26].

The ECA is characterized, besides the CLLJ, by other low-level wind streams: the Chocó jet (CJ) [24] in the ETP, the jet over the Venezuelan Llanos [46], and the so-called gap winds along Central America [23,34,35]. These strong currents have significant relevance to local circulations such as sea breezes [47], intense convective activity, and regional precipitation distribution. The CJ located near Colombia, is composed of winds that are colder and moister than continental air. The season of strongest winds is October-November, being February-March their weakest period. This jet is an extension of the southeasterly trade winds of the Southern Hemisphere that is generated by the ocean-land temperature contrast, by a shallow baroclinic layer over the Pacific Ocean and the Coriolis force, the last two, acting to turn the circulation towards the land [24]. This current is associated with strong convection and moisture transport interacting with the ITCZ, and the topography gap in the western branch of the Andes [24].

Tropical cyclones are also prominent systems in the production of convection and lightning activity, however, very few studies have been published in this regard for the ECA region accounting for their contribution to lightning strokes. A recent study reported the case of Hurricane Otto, which reached category three (Saffir-Simpson Scale) to the east of Costa Rica and Nicaragua, breaking several historical records in 2016 [15]. This cyclone was the strongest hurricane on record so late in that year, the latest hurricane on record to be located in the Caribbean Sea, and the only known hurricane to move over Costa

Rica [48]. A significant amount of lightning activity (a known proxy for convection), was for the first time documented for a hurricane near Central America [49]. A more detailed study about the distribution of lightning activity associated with the evolution of Otto can be found in [15].

Gap jets are also observed in the ECA, being the most important, and also the Panama, the Papagayo, the Gulf of Fonseca, and the Tehuantepec jets. There are different physical mechanisms explaining these features. Southward-moving cold fronts produce strong pressure gradients between the Caribbean region and the eastern Pacific [38,41], so the wind is channeled through topographic gaps in those sectors [23,34,35]. The winds can be very strong as reported by [50]: "during a northern wind associated with the Tehuantepec Jet, one ship 3 km offshore in the Gulf recorded a sustained wind of 50 m/s with gusts up to 60 m s^{-1}." In the case of the Papagayo Jet, [23] showed that winds associated with this jet can reach values in excess of 22 m s^{-1} for Managua (Nicaragua) and Liberia (Costa Rica) at levels near 1500 meters above sea level, using data from the Pan American Climate Studies/Sounding Network [51]. Note the strength of the vertical wind shear over that region. The winter feature of the latter jet has been proposed as the forcing mechanism for the Costa Rica Thermal Dome [52–54]. The Gulf of Fonseca jet (barely known or studied) has been described by [34,35] as having potential to maintain a gap flow during boreal summer and winter months. The importance of the gap winds within the frame of this work resides in the fact that strong low-level currents tend to inhibit convection and associated thunderstorms and lightning activity on the Pacific hillsides of Central America related to the strength of the vertical wind shear.

In regard to the role of sea surface temperature (SST) to regional convection, it is relevant to name the Western Hemisphere Warm Pool (WHWP) system [36,37]. The two components of the WHWP develop, one in the Gulf of Mexico and the Caribbean, and the other in the ETP. Regional convection and the rainy season are influenced by the two components of the WHWP, which are out of phase, migrating, and changes in size depending on small temperature variations [34,35]. In regard to the structure and multiscale interaction amongst some of these systems, ref. [34,35] offered a review of their basic dynamics and the associated modes of variability, including those of systems in the ETP.

Diurnal land-sea breezes are also relevant modes of mesoscale circulation in this region, however, convective activity and potential lightning variability depend on the interaction of local winds with the trade wind system, especially with the seasonal strength of the Caribbean Low-Level Jet. A recent study of sea breeze (SB), using observations in the Pacific coast of Costa Rica, showed that observed precipitation was a maximum between 14:00–17:00 LST, in agreement with local diurnal heating and the development of convection [47]. Data comprised the period of 1 July to 16 September 2004 from Ticosonde-North American Monsoon Experiment, and a local University of Costa Rica-National Meteorological Institute field campaign. That was the first study in which observations and numerical modeling were used to analyze the dynamics and mechanisms of SB in the climate of Costa Rica. The analysis of two particular periods during a strong (weak) flow of the CLLJ exhibited a less SB development during the former, which suggested the strong influence of the CLLJ on local rainfall regimes and local processes such as the SB and potential lightning. These results also apply in general for the Caribbean coast of Costa Rica [43].

3. Data and Procedures

The ECA region is an atmospheric system showing a complex dynamical multiscale interaction between atmospheric modes, and it is worth investigating, especially since most of them are far from being completely understood. However, there are limitations in observed data for accomplishing that target. For instance, sound data for a more realistic atmospheric analysis has fallen in frequency and in quality during the past 3–4 decades. Besides that, the meteorological surface observation network is far from being uniform, both in space and time, especially near coastal areas, and the Caribbean slope of Central

America [44], outlined some of these limitations in data availability and data processing). Here we see WWLLN data as an opportunity to study some of the ECA atmospheric climate signals using remote sensing information that reanalysis data does not usually provide. In this respect the findings of [55] are very suggestive and allow researchers the use of WWLLN information as a basis to construct climatologies to resolve diurnal and seasonal variations of atmospheric fields.

The WWLLN started circa 2004 with 18 stations globally, grew up to 20 stations in 2005 [56], and to nearly 60 stations by 2012 [57]. According to the last authors, the more stations were in place, the better the WWLLN's ability to detect even weaker strokes. We are aware that the detection efficiency of the network also varies due to the non-uniform sensor spacing over the world. However, [57] also pointed out that the network improved in accuracy and detection efficiency with an increase in the number of stations (i.e., the increase from 11 stations in 2003 to 30 in 2007 led to a rise of 165% in the number of lightning strokes detected). In their work they used about 14 stations in the Americas, in contrast to the current 25 active sensors for the same región, an increment of about 30% in the number of stations in the last 9 years, approximately. Moreover, detection of strokes does not depend exclusively on nearby sensors. According to [56] "the propagation of sferics (very long electromagnetic wavelengths up to 100 km), allows lightning strokes to be located in real time at up to 10,000 km from the receivers with a location accuracy that is estimated to be a few km". Regarding the location accuracy [58] estimated to be in the order of 10 km. In our paper, we have assumed, following the 10,000 km argument, that the data we used for the ECA region depends on sensors as far as North America, South America and some parts of Europe. In the Americas there were only 4 stations in place in 2006 [58], by 2012 the number had increased to 13 sensors (including our station at the University of Costa Rica) [57], and by 2021, the WWLLN reports nearly 25 stations in operation (https://wwlln.net/ accessed on 28 December 2021). Based on the above data we considered that the best record to use here was that of 2012–2020, with the detection efficiency varying little from year to year since the number of stations (25), in general, remained operationally for most of that period over ECA (Figure 1).

The WWLLN detection efficiency has been a concern since the early days of this network [58]. At that time WWLLN had about 25 stations globally. Although the relatively small number of sensors across the world, [58] analysis showed that when compared with a lightning location network operating in New Zealand, discharges with larger currents were observed by more stations across the global network. The detection efficiency, however, presented strong spatial variations depending on the station density. In [58] the authors calculated the relative detection efficiency for a network having uniform detection sensitivity to correct for regions with less sensors and variations in atmospheric very low frequency wave propagation. One of their results was that WWLLN has a bias toward detecting low-energy strokes over oceans rather than over land. In their work differences in the intensity of convective activity were not considered, a factor that plays a relevant role since it depends on topography and location, especially in tropical areas such as the one studied here. According to [55] the global detection efficiency of WWLLN is ~10% for all strokes, supplying basic lightning information for diurnal and seasonal climatologies. WWLLN reports that "recent research indicates our detection efficiency for strokes about 30 kA is approximately 30% globally". More recently, [59] stressed the fact that in the early stages of the network (before 2008), the detection efficiency was low because there were only a relatively small number of sensors. Lightning efficiency has been monotonically increasing since the early days of the network [58], by a factor of about 1.25 (60 in 2012, [58]; to over 70 in recent years, http://wwlln.net/ accessed on 28 Decmber 2021). Studies have also used some sort of adjustment factors for WWLLN D based on the LIS/OTD (Lightning Imaging Sensor, LIS, and Optical Transient Detector, OTD) climatology [59], although LIS/OTD has a quite different detector sensor detecting pulses of illumination (produced by lightning) above background levels.

Estimates of precipitation have been possible due to satellite monitoring programs such as the Tropical Rainfall Measuring Mission (TRMM, https://gpm.nasa.gov/missions/trmm, accessed on 28 December 2021), the Global Precipitation Measurement (GPM) mission https://gpm.nasa.gov/missions/GPM, accessed on 28 December 2021), and CHIRPS (https://www.chc.ucsb.edu/data/chirps, accessed on 28 December 2021), a project using rain gauge and satellite observations. As mentioned before, precipitation in CA is mostly of convective character, so its prediction, both qualitative and quantitative, is a crucial element to diminish socioeconomic impacts in a region with a weak economy. Besides TRMM, GPM and CHIRPS data, the question whether other global networks such as the WWLLN can provide multiscale information for convection and precipitation esti mates is yet to be investigated. As reported by [55], "though no single lightning climatology can be said to be definitive, the WWLLN lightning climatology appears to be consistent with in situ rainfall observations and with the TRMM rainfall climatology". Following [59] when discussing TRMM satellite studies, we considered that by estimating monthly or annual lightning averages for the period 2012–2020, the gross statistical characteristics of the lightning-precipitation patterns will emerge.

On diurnal scales, several works have indicated that the evening maximum lightning over the continent (i.e., South America) and oceanic basins are consistent with those of precipitation in regard to phase propagations [60]. As also reported by [61], lightning–lead precipitation relationship is also seen between TRMM3G68 precipitation and WWLLN lightning around Central America. Other results [61] indicate that WWLLN amplitudes are large over the oceans and around Central America. The above two outcomes provide reliability to our research and results. The authors realize that although the availability of TRMM, GPM, CHIRPS, satellite and lightning network data, estimates of the phase relationship between convection, precipitation and lightning is not an error-free problem. All the above data sets have shown biases with respect to observations when available. This issue is also present in numerical models [62], when they argue that in their work's context: "errors are often the result of a number of interacting biases". We think that this is the case for the relationship between convection whether natural or forced, precipitation, and lightning data, especially with the known location uncertainties and relatively low detection efficiencies in some parts of the world. One additional point worth raising here is the difficulty to deal with short time and space scales (i.e., sea breeze) versus longer time and space scales (for instance, seasonal climate signals). The lightning area average appears to be a good proxy to represent precipitation on seasonal and longer time scales. These authors were in favour of investigating that relationship here, since the MSD, the CLLJ, the ITCZ, and other tropical systems in this region, have clear climate signals on precipitation that "lose" their identity for short time scales.

The lightning data used in this study is a subset of the daily information gathered and run by the WWLLN (http://wwlln.net/, accessed on 28 December 2021). The Center for Geophysical Research (CIGEFI, in Spanish) at the University of Costa Rica has been one of the WWLLN monitoring stations since 2008. This study analyzed daily data to produce monthly and annual averaged information in order to investigate the time and space structure of lightning in the ECA from January 2012 to December 2020. Although the WWLLN has data from 2006 to present (approximately), the average number of sensors at the beginning of the network was relatively low (Figure 1), so data had more uncertainty in the location of discharges than that of the period P used here (2012–2020). The WWLLN provides mainly cloud to ground continuous lightning detection coverage over the entire globe, though the dataset considered here was delimited to the ECA, the region of study shown in Figure 1 (inserted panel). The process to identify the hot and cold-spots of lightning activity (both defined in next section) in the ECA region is as follows. A variable containing information on spatial and temporal lightning density over the ECA was defined. Lightning data for each daily window were compiled into gridded areas with a fixed resolution of 15 km by 15 km. For this, it was assumed that the uncertainty area in the lightning location was of the order of 5 km by 5 km [13,56,58], so the total number of

lightning strokes within a given area of 225 km^2 was assigned to the central grid point designed here, in general, as an (i, j) point. No intersection of areas was allowed, so a lightning stroke is only counted once in a given grid area. The total area of analysis (Figure 1) has an approximate dimension of 3850 by 2770 km, so, the number of points in the grid data are, in the "x" (eastwards, with index "i"), and in the "y" direction (northerly with index "j"), 257 × 185 grid points, respectively.

The daily lightning number of strokes in every grid box [$n_{i\,j}$] for all days of a particular month m was aggregated to obtain the total number of strokes [$n_{i\,j}$] $_{m\,k}$ for every month (m = 1, . . . ,12), of every year k (k = 1, ...9) of the period P. A simple averaging process was applied to get the monthly mean values, and the yearly mean values, as appropiate. The lightning density D variable at position (i, j) was defined as,

$$[\ D_{i\,j}\ ] = [\ n_{i\,j}\ ]\ [\ a\ ]^{-1}$$

In the above expression, i = 1, . . . , 257; j = 1, . . . , 185; and "a" is the fixed grid area of analysis (225 km^2). The lightning density D units are then, the number of lightning strokes N km^{-2} $month^{-1}$ or N km^{-2} $year^{-1}$, depending on the variable to be estimated.

Figure 1 (bars) shows important differences in the total yearly number of WWLLN sensors, and as a consequence, in the total number of strokes from year to year in the ECA, for the period 2006–2020, so a climatology based on all available data would most probably be very biased, as discussed before. For that reason, the period of analysis was shortened to 2012–2020, where variations from year to year were a minimum and the number of sensors remained nearly constant. When the climatology was obtained for 2006–2011, the D were significantly smaller than those of the period 2012–2020 considered here (not shown). To complement the analysis of lightning data with other atmospheric variables, such as precipitation, ERA5 data was used. ERA5 is a product of the European Centre for Medium-Range Weather Forecasts that provides global, hourly estimates of atmospheric variables, at a horizontal resolution of ~30 km, with 137 vertical levels from the surface to 0.01 hPa, from 1979 to present (https://climatedataguide.ucar.edu/climate-data/era5-atmospheric-reanalysis, accessed on 12 May 2021).

4. Results

WWLLN detected a total number of 5 × 10^8 lightning strokes, approximately, during the 2006–2020 period over the ECA (Figure 1). The annual count of electrical discharges varied significantly from year to year, especially during the period 2006–2011 due, as explained above, to the relatively small number of WWLLN sensors, both globally and within the ECA region during those years.

It can be seen from Figure 1, that the network increase in lightning detection in the ECA region is coherent with the WWLLN number of sensor growth, globally. Nowadays, WWLLN has over 70 sensors worldwide. The seasonal distribution of the lightning strokes shown in Figure 1 by month and for all years, indicates that the number of flashes during the most widespread wet season (September–October) is about one order of magnitude greater than that during the regional (mostly) dry season (January–February–March). During the latter months most of the share in lightning activity comes from cold surges entering the tropical regions [39,40,42].

The overall regional effect of the MSD, being a reduction of convective activity and precipitation in the Pacific side of the region [23], is visible only in some years of the 2012–2020 period during July–August, assuming lightning means are a proxy, especially for the climate distribution of precipitation. In Figure 1 that characteristic is shown as a reduction of the total number of lightning strokes, especially during the above two months. Discussion on this feature is retaken below where D are separated for the Caribbean and Pacific basins using a subjective criteria involving the highest mountain peaks in the region analyzed. The inserted panel in Figure 1 gives an idea of this natural separation. The work of [9], also used WWLLN data and separated the information in Chile regionally to study its seasonal variability.

Figure 2 presents the monthly average of lightning activity (number of strokes km^{-2} month^{-1}) over the ECA region for 2012–2020. The season with the least activity corresponds to the winter months in the Northern Hemisphere (December–January–February), a period characterized by an ITCZ located in its southernmost position near 5–6° N. In the mean, March–April is a sort of transition period to a more spread wet season that runs from May to November. For some regions the minimum activity, as will be shown below, is connected to the summer dry season (MSD) in several locations in the ECA, especially over the Pacific inclines of Central America and southern Mexico. The first maximum of lightning activity appears in March, and as indicated before, is associated with the northern migration of the ITCZ over the ETP. The second mean peak of electrical discharges appears in September-October. This maximum is a result of a more vigorous convection pattern associated with the widespread regional wet season, which in turns, is the atmospheric response to a weakened trade wind-shear over the CS and associated generation of tropical cyclones [48], to traveling disturbances such as tropical and easterly waves [23], and to a moisture transport from the CS to Central America and southern Mexico [26]. Some of the above results are consistent with the findings of [63] for the Mexican Plateau, where it is reported that "the seasonal variation indicates that the lightning flash peak currents were found to be larger in summer with less than 10% occurring in the autumn and winter".

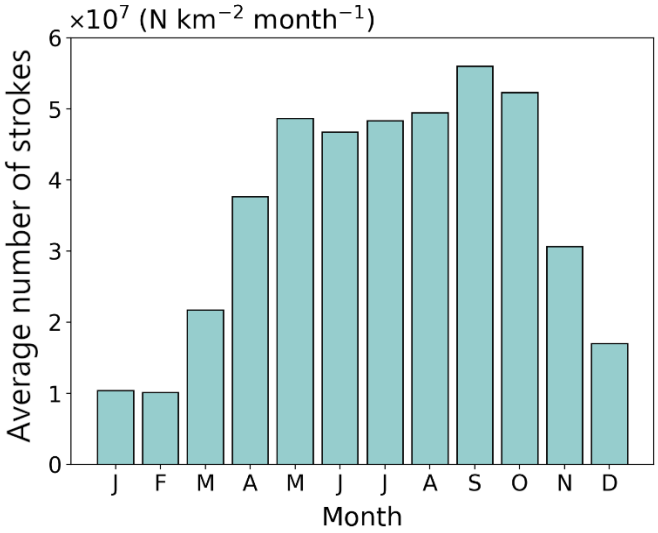

Figure 2. Average monthly distribution of lightning activity (total number N of strokes km^{-2} month^{-1}) over the Extended Central America region for 2012–2020. Data from the World Wide Lightning Location Network (WWLLN).

The monthly average of lightning density distribution in the ECA is shown in Figure 3. The regions with the largest lightning density (named here "hot-spots"), using the density magnitude in ascending order are: the Panama Bight in Panama (PB; D~21.84 N km^{-2} year^{-1}); the Central Pacific of Costa Rica (CP; D~23.45 N km^{-2} year^{-1}); the Gulf of Fonseca between El Salvador, Honduras and Nicaragua (GF; D~25.18 N km^{-2} year^{-1}); Tehuantepec in Mexico (T; D~26.11 N km^{-2} year^{-1}); Escuintla in Guatemala (E; D~37.57 N km^{-2} year^{-1}) and the Gulf of Maracaibo in Venezuela (GM; D~40.82 N km^{-2} year^{-1}). This last finding of a regional maximum of lightning strokes in the so-called region of the "Relámpago del Catatumbo", is notoriously consistent, except for its density values, with the works of [12,29]. As reported by [12], the Lake Maracaibo Basin in north western Venezuela has the highest annual lightning rate of any place in the world (~200 N km^{-2} year^{-1}), using the LIS/OTD satellite data for north western South America, which is more than four times the density found here for the same region. Differences may be due to the fact that the WWLLN is good at detecting mainly cloud to ground lightning [55], while the data managed by [12] contains both, cloud to ground and intra-cloud lightning.

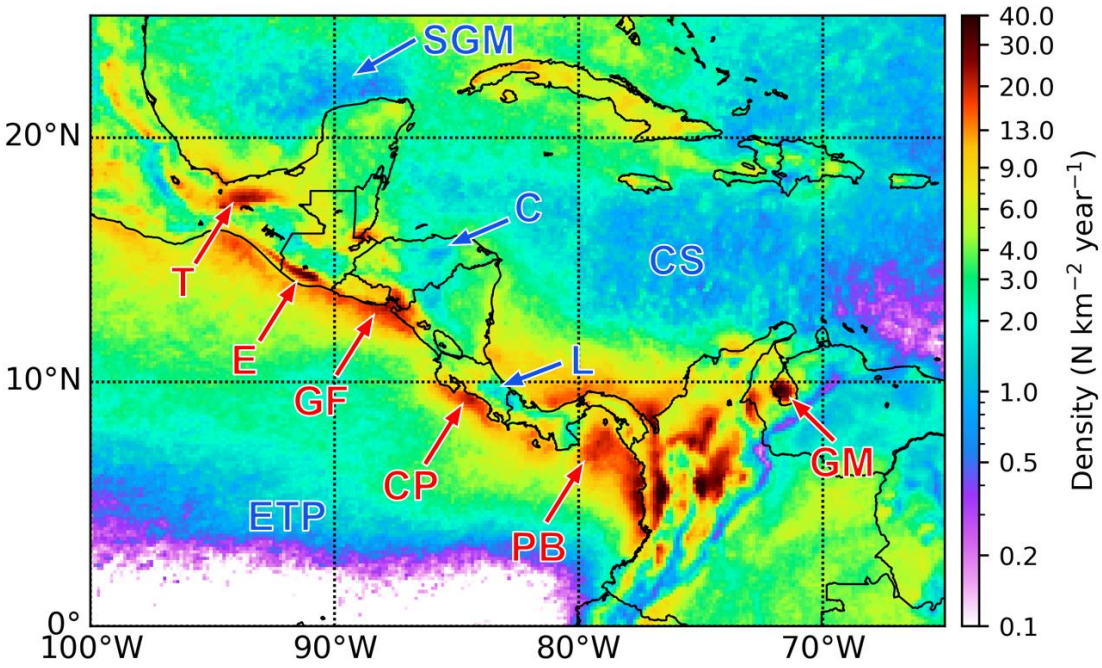

Figure 3. Annual average density of lightning activity (total number N of strokes km^{-2} month^{-1}) over the Extended Central America region 2012-2020. Major lightning hot-spots are in Tehuantepec (T), Escuintla (E), Gulf of Fonseca GF, Central Pacific (CP), Panama Bight (PB), and Gulf of Maracaibo (GM). Major lightning cold-spots are in the southern Gulf of Mexico (SGM), Colón (C), and Limón (L). ETP and CS stand for the eastern tropical Pacific and the Caribbean Sea, respectively. Data from the World Wide Lightning Location Network (WWLLN) for 2012–2020.

A recent work [64] identified several lightning hotspots in Central America using observations from LIS. Two of them are in Guatemala, near Patulul (14.35° N, 91.15° W) and Catarina (14.85° N, 92.05° W), and the other in Honduras near San Jerónimo (13.15° N, 87.25° W). In this work just one whole hotspot is observed nearly parallel to the coastline in Guatemala in the Escuintla region, and the other in Honduras right in the Gulf of Fonseca (Figure 3), where there is a mangrove of regional ecological importance [65], a relationship pointed out by [21]. In the former work, all hot-spots in Central America appear to have a pronounced continental signal, while in this research the spots are located nearer or over the maritime areas. Lightning activity in this work is very pronounced over the nearby oceans of ECA (Figure 3), contrary to the findings of [64] using a very high-resolution (0.1°) total (cloud to ground and intra-cloud) data from LIS observations. Our results, however, are consistent with the results of [30] that reported using WWLLN information over marine regions near Mexico, that D were often as high as that observed over the continent. This pattern, although for a different period than the one used here, is observed in Figure 3, especially in the stroke density contrast between Tehuantepec and the southern and southwestern Gulf of Mexico.

Regions with the lowest lightning density, named here "cold-spots", are located in the southern Gulf of Mexico (SGM), in northern Nicaragua and near Colón in Honduras (C) and southern Limón province in Costa Rica (L), including northern Panamá and the Azuero Península. Some areas of low D are also observed in central Guatemala and southeastern Mexico. As the data revealed, hot-spots are mainly located in the Pacific hillsides of the ECA, except in the central SGM. Most cold-spots are located in the Caribbean side of Central America, which paradoxically, is a region with strong convective activity for a good part of the year due to tropical cyclones, waves and other travelling atmospheric systems. One striking characteristic of the D distribution in ECA is the strong horizontal gradients of this variable in some regions of ECA (e.g., the CP and L in Costa Rica). The existence of the CLLJ core near its mean position close to 15° N and 70–80° W [21,32,33],

and its extension toward the northwest confirm the importance of this current to reduce, on average, convection in that region via a strong vertical wind shear and possibly as a reduction in SST [23]. This regional climatological imprint of the CLLJ on the lightning activity had not been reported before.

Figure 4 presents the average monthly lightning density over the ECA for 2012–2020. January–February–March is the season with the lowest lightning density over most of Central America and southern Mexico (Figure 4a–c), coinciding with the highest tourist season of the region. Low to medium densities of about 0.2–1.5 N km^{-2} month^{-1} are observed in southern Costa Rica and the Panama Bight as a result of trade winds transporting moist air from the Southern Hemisphere reaching tropical areas during those months. The ITCZ in the ETP begins to clearly migrate northward in March (Figure 4c). April (Figure 4d) is a sort of a transition month to a more widespread regional lightning activity in the Pacific associated with the ITCZ northward migration. In the Caribbean, travelling disturbances from the east favored convection continuing its activity during May–June (Figure 4e,f). During May (see Figure 4e), D density increases over the ECA associated with intense convection in the WHWP and the northern migration of the ITCZ; this being the beginning of the rainy season with the first peak in June [23]. Figure 4e also displays widespread lightning activity over Mexico and high D over the Isthmus of Tehuantepec influenced by the Tehuantepec Jet. As explained by [30], northerly winds go through the narrow mountain of the Isthmus reaching a warmer than normal SST over the Pacific during that season.

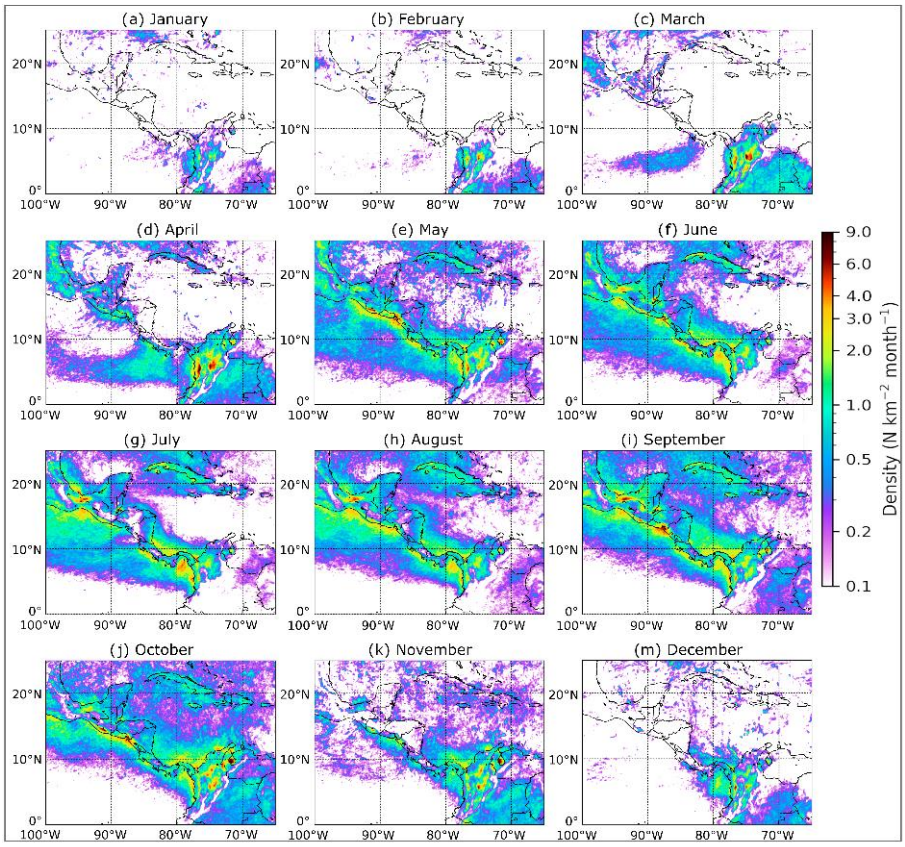

Figure 4. Average monthly lightning density (N km^{-2} month^{-1}) over the ECA for 2012–2020. Data from the World Wide Lightning Location Network (WWLLN).

July (and to a lesser extent August) shows a marked decrease in lightning activity associated with the MSD, especially over parts of the Pacific slopes of Central America and southern Mexico (Figure 4g,h). According to [57], the start, minimum, end, intensity and magnitude of the MSD is quite variable. These authors also report the need to create

indexes representing the timing of the MSD phases for regional prediction, something that the lightning strokes, as a proxy, may help with. June-July-August is a season with a notable increase in the intensity of the trade winds linked with the development of the CLLJ. This strong current during the summer months acts as a lid inhibiting convection due to its strong vertical shear during this season [23]. It is remarkable the form in which the CLLJ imprints the Caribbean with a large region of minimum lightning activity (Figure 4g–i), regardless of the generation of tropical cyclones and traveling waves during that period [34,35]. Figure 4g for July shows the effect of the vertical wind shear associated with the CLLJ and its extension across the Gulf of Papagayo, inhibiting convection and considerably reducing the D over that region and the ETP. According to this data the MSD in this region in front of Papagayo extends westward into the ETP for at least 400-450 km. Some other regions of Central America present a reduction in D as a result of the same physical process, a characteristic of the MSD [25]. To complete the analysis Figure 5 is presented. This figure shows a high physical coherence between the D and the structure and nature of the CLLJ, and its associated vertical wind shear over the region, as measured by the mean July wind at 925 hPa for 2012–2020, especially over the CS and parts of the ETP. Another interesting result of this work, observed in Figure 5, is the relation of the region where the CLLJ has a maximum intensity in the central CS, in general, across the Yucatan and the Gulf of Mexico during the boreal summer months to the low values of D over the corresponding areas of EC (Figures 4f–k and 5). The appearance of higher densities over the oceans (Figure 4f–j) is remarkably coherent with the monthly distribution of tropical cyclones, both in the CS and the ETP [34,35].

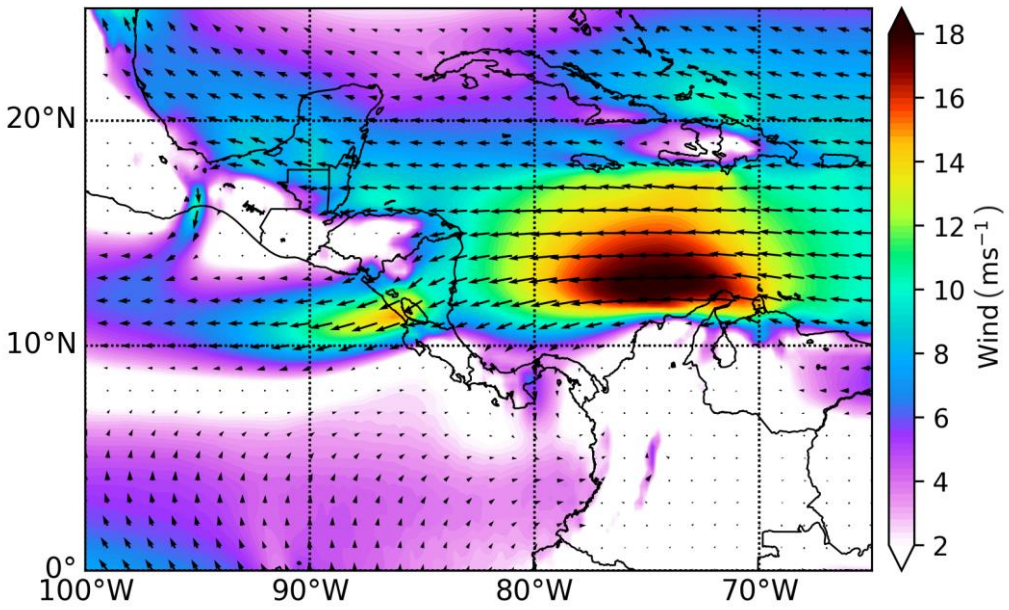

Figure 5. Average July monthly wind speed at 925 hPa from ERA5 over the Extended Central America for 2012–2020. (https://climatedataguide.ucar.edu/climate-data/era5-atmospheric-reanalysis, accessed on 12 May 2021).

It is also noted here that there are two regions with high D in northwestern South America. One of them is in Colombia near the El Chocó region associated with the intensity peak of the CJ during October–November (Figure 4j,k). The other one is located in the tropical zone of "Catatumbo", an area with the highest lightning activity worldwide [12,29], that reported a density of about 53 N km^{-2} year^{-1}, using a Lightning Mapping Array system. Although there are differences in the sensor properties, that value is relatively close to the one found here of 40.82 N km^{-2} year^{-1}. September–October (Figure 4i,j) is a secondary maxima of lightning activity; the Pacific coast having a higher density, where mountain ranges are sharp near the coastline increasing, by orographic forcing and

incoming radiation, thunderstorm activity and associated precipitation. The CS has the second rainfall maxima during September; Cuba and Costa Rica's Caribbean coast showing high lightning activity related to the weakness of the CLLJ vertical wind shear and to the traveling disturbances during this season. During November–December (Figure 4k,m), the lightning activity starts declining over the Pacific and Caribbean coast; these months being part of the transition period to a more dryer season with stronger than normal trade winds over most of the ECA and cold northerlies dropping the sea surface temperature and inhibiting convection [23].

A simple estimate of the contribution to D regional seasonal distribution from the CS and the ETP basins is presented in Figure 6. For this, a straightforward topographical separation procedure was done observing the annual mean distribution (Figure 3) of D over the ECA. As this figure shows the mountain ranges across the ECA appear to be a kind of natural separator for D. To construct Figure 6, an approximate line was delineated taking into consideration the highest mountain peaks across the region (see inserted panel in Figure 1 for topography). First of all, Figure 6a exhibits a great degree of variability in D, both intra seasonally and annually; this result being coherent with the variance of atmospheric systems during some seasons (e.g., easterly waves and tropical cyclones). During the boreal winter, it is very clear the contribution to D coming from cold fronts entering the low-latitudes. September–October peaks in D, whereas during the summer months there is a reduction associated with the development of the CLLJ, its strong vertical shear in that region inhibiting widespread convection. Figure 6b displays a different behavior of LD over the ETP, partly due to the high contribution of the ITCZ in the total counting. The seasonal and inter-annual variability of the ETP is greater than that of the CS basin, showing years with very intense lightning activity (e.g., 2012, 2015) and others with relatively lower conditions. No clear signal of the MSD is observed in Figure 6b; its masking is most probably due to the predominant contribution of the ITCZ.

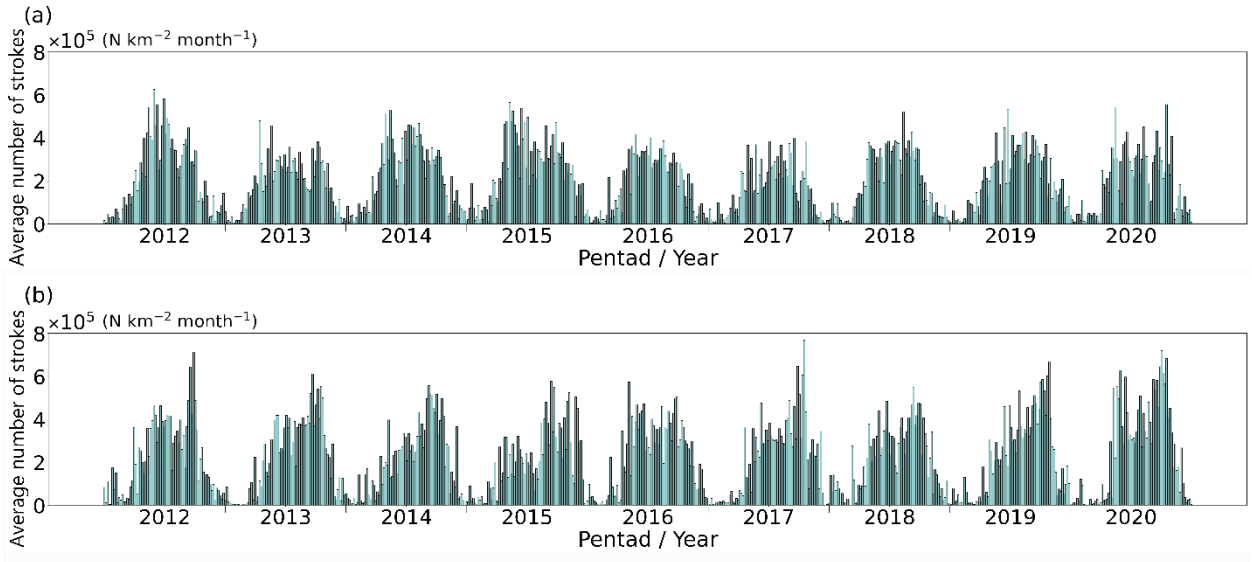

Figure 6. Average monthly distribution of lightning activity (total number of N km^{-2} month^{-1}) over (**a**) the eastern tropical Pacific, and (**b**) the Caribbean Sea using the World Wide Lightning Location Network (WWLLN) data each year of 2006–2020.

5. Discussion

According to [23], the seasonal precipitation distribution along the Pacific slope of Central America and southern Mexico shows a reduction during July–August (the MSD), with peaks in June and September-October. Since lightning is a proxy for convection and precipitation, regions with minimum D values could be associated with the MSD signal in the above region. During its development and duration, other atmospheric

parameters such as, radiation, wind, moisture content, and ground and ocean surface temperature must be coupled with their covariability, the precipitation field. In order to offer a plausible explanation on the observed seasonal lightning distribution obtained here and its association with the MSD in some regions (see Figure 4g,h, where this a predominant feature; e.g., northern Costa Rica and southern Nicaragua), the following physical mechanisms are proposed to couple land-ocean-atmosphere processes. During July-August strong winds associated with the CLLJ cross Central America between Costa Rica and Nicaragua reaching the ETP (Figure 5 in this paper, and Figure 8a in [23]). A consequence of this process is to reduce the SST over that region by means of surface drag and eddy-like features of wavelength 600 km propagating southwestward [66]). Besides this, the CLLJ is characterized over that region just westward of Costa Rica and Nicaragua, by a strong vertical shear (see Figures 6a and 7b in [23]), a factor also reducing convection. These two physical processes are consistent with the findings of this work for a minimum of D during July-August in that region. Following that reasoning, on average, during the previous period to the onset of the MSD (June), the short wave radiation (SWR) reaching the ground should be a relative minimum, since there is a deep convective cloud coverage accounting for the maximum rainfall during that month. This is a pattern that can also be invoked for September-October. During the MSD, a minimum of convective cloud coverage may explain the precipitation reduction from June to July-August, and the SWR must be a sub-seasonal relative maximum. According to this basic idea, the surface temperature may have a distinct diurnal range depending on the seasonal evolution of precipitation. So, during June, maximum temperature (Tmax) over the continental area should be smaller than during the MSD just due to less incoming SWR, while the minimum temperature (Tmin) should be greater than that of the MSD due to a relative maximum of cloud coverage. On the contrary, the MSD should show a larger diurnal range than that of June, since more SWR is reaching the ground, and with less convective cloud coverage in the mean and, the outgoing long wave radiation (OLR) must be greater than that of June.

To simply test the above relationships between Tmax, Tmin, convective precipitation, and lightning in that region, Figure 7 was generated. This figure shows ERA5 data for the period June–July–August (2012–2020) for a single grid point near 11° N, 86° W located between La Cruz (Costa Rica), and San Juan del Sur (Nicaragua), assuming that it is representative of mean conditions for the near a land-continental area. Anomalies were estimated following the standard procedure and pentad values (5-day periods) begin in June (pentad 30), and end in August (pentad 48). All pentad averages for all variables were estimated using ERA5 and WWLLN data at the 15 × 15 grid-box area defined above for the period 2021–2020. As can be observed in that figure, the precipitation anomalies are positive during pentads 30 to 33–34 corresponding approximately to the third week of June and to the first peak of the rainy season. During this period D is a relative maximum. Negative precipitation anomalies are present from pentads 34–35 to 45 approximately, corresponding to the interval from late June to mid-August approximately, when D is a minimum. This phase of the precipitation pattern has been associated with the MSD. After pentad 46, Figure 7 shows the beginning of the second rainy period in that region, so lightning increases. With respect to extreme temperatures, Tmax and Tmin behave in agreement with a relatively long interval of negative precipitation anomalies (pentads 34 to 42), after which on average, Tmax raises and Tmin diminishes for at least 3–4 pentads. Although this is not conclusive, it brings attention to test the proposed mechanisms with observed data for a larger area in the future.

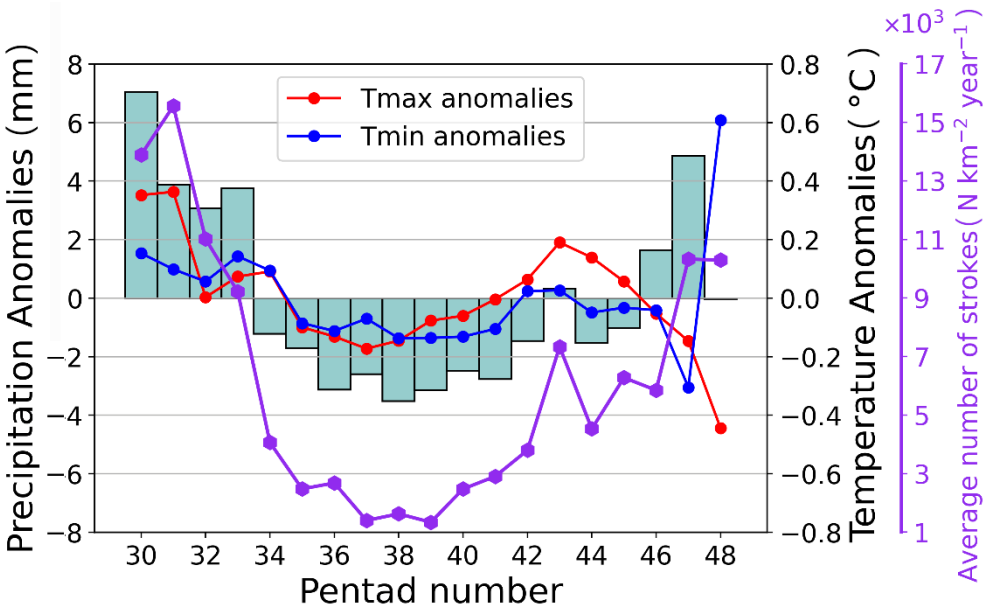

Figure 7. Lightning density, precipitation and extreme temperature anomalies at a single grid region (circa ~225 km^2, near 11° N, 86° W) located between La Cruz (Costa Rica), and San Juan del Sur (Nicaragua). Data from ERA5 (precipitation, extreme temperatures) and WWLLN (lightning density) for the period 2012–2020. (https://climatedataguide.ucar.edu/climate-data/era5-atmospheric-reanalysis, accessed on 12 May 2021).

6. Conclusions

The lightning activity over the ECA using WWLLN data was analyzed for 2012–2020 showing that it is highly dependent on the orographic forcing, the climate characteristics and season of the year. Mainly three regions show high lightning density over Mexico: Sierra Madre Oriental, Balsas River, and the Gulf of Tehuantepec. The seasonal distribution of lightning strokes shown in Figure 1 by month and for all years, indicated that the number of strokes during the regional (mostly) wet season (September–October) is about one order of magnitude greater than that during the regional (mostly) dry season (January–February–March). During the latter months most of the share in lightning activity comes from cold surges entering the tropical regions. There is a remarkable regional effect of the MSD over the ECA, observed as a clear reduction of lightning activity in some years during July–August for 2012–2020; this characteristic being especially dominant over the Pacific inclines of Central America and southern Mexico. The findings of this work are consistent with other already known hot-spot regions, such as the Catatumbo and northwestern South America, however, the densities found in this research are lower than those of [12,29]. Differences may be due to the fact that the WWLLN is good at detecting mainly cloud to ground lightning [55], while the data managed by the above authors contains both, cloud to ground and intra-cloud lightning with high resolution data of LIS and OTD observations. According to [64] all hot-spots in Central America had a continental signal, while in this research, these features are found mainly over the oceans near to coastlines. As the data revealed, hot-spots are mainly located in the Pacific inclines of the ECA, except in southwestern Mexico. Most cold-spots are situated in the Caribbean side of Central America, which paradoxically, is a region with strong convective activity for a good part of the year due to tropical cyclones, waves and other travelling atmospheric systems. The importance of pointing out the cold-spot regions resides in the fact that low D implies a minimum of vulnerability to human impacts and many industrial developments. July (and to a lesser extent August) shows a marked decrease in lightning activity due to the presence of the CLLJ (its vertical wind shear) and the development of the MSD, especially over parts of the Pacific inclines of Central America and southern Mexico.

The CLLJ acts as a lid inhibiting convection due to its strong vertical wind shear during the boreal summer months [23]. The convective inhibition is mainly due to the climatology wind shear distribution. This shear as pointed out by [67] is not explained by the observed meridional sea surface temperature gradient, so baroclinicity can be ruled out as opposed to the African Easterly Jet [68] showed that the CLLJ is barotropically unstable in that region [22], so energy could be exchanged between mean flow and disturbances. The CLLJ entrance is observed in the easternmost part of the CS, where descending motion dominates and precipitation is a regional minimum [23,44]. (2014). The jet exit is found near the Costa Rica-Nicaragua border, a place of strong convection and a regional maximum of precipitation [22,44], and some references therein) that coincides coherently with lightning densities over that region. The CLLJ has a long term maximum of over 12–14 m/s near 925 mb showing a strong vertical wind shear that inhibits convection during summer [23] This feature is also observed in Figure 5. In situ sounding observations taken just north of the mean CLLJ core position at 15° N during a field experiment named "Experimento Climático en las Albercas de Agua Cálida (ECAC Phase 3) campaign in July 2001 confirmed such a strong wind shear and a poor convective regional activity associated with the strength of the CLLJ [23].

Another interesting result of this work is the negative influence of the CLLJ to lightning activity, both in the region where is observed to have a maximum in the central CS during the boreal summer months, and in the region to the northwest of it, across the Yucatan and the Gulf of Mexico (Figures 4f–k and 5). Figure 4g shows the effect of the CLLJ vertical wind-shear and its extension to the Gulf of Papagayo, diminishing convection and considerably decreasing the D over a region extending westward into the ETP for at least 400–450 km. The proposed simple physical mechanism to account for the coupling between the CLLJ and the MSD needs to be tested in more depth by including observed data for a wider region. Based on previous work, we consider that our results very likely also have information on the influence of the diurnal cycle of atmospheric modes on lightning, unfortunately, such a topic was not touched in this paper and needs further consideration. A study including the relationship of land-sea-breeze circulation with convection, precipitation and lightning, would be very valuable to gain insight into these processes at low-latitudes. Although the WWLLN data record is relatively short to study other regional atmospheric signals in the region, it would also be interesting to investigate the interannual variability of lightning associated with El Niño-Southern Oscillation phases in the near future. Last but not least, our results on the regional distribution of hot and cold-spots of lightning activity in the ECA, have notable implications for safer touristic activities, better agricultural and fishery practices, and suggest that WWLLN data could also serve as a proxy for precipitation distribution at different time scales, just to mention a few of them.

Author Contributions: Conceptualization, J.A.A. and D.A.-F.; methodology, J.A.A. and D.A.-F.; software, J.A.A. and D.A.-F.; validation, J.A.A. and D.A.-F.; formal analysis, J.A.A.; investigation, J.A.A. and D.A.-F.; writing—original draft preparation, J.A.A.; writing—review and editing, J.A.A.; visualization, J.A.A. and D.A.-F.; supervision, J.A.A.; project administration, J.A.A.; funding acquisition, J.A.A. All authors have read and agreed to the published version of the manuscript.

Funding: The authors wish to acknowledge the funding of this research through the UCR- Vice-Presidency for Research Grants VI-805-A4-906/A5-719/B0-810/B5-296/B8-604//B9-454/B9-609).

Institutional Review Board Statement: Not applicable.

Informed Consent Statement: Not applicable.

Data Availability Statement: WWLLN data is available at https://wwlln.net (accessed on 28 December 2021). ERA5 data is available at https://climatedataguide.ucar.edu/climate-data/era5-atmospheric-reanalysis (accessed on 28 December 2021).

Acknowledgments: This research was supported by the Center of Geophysical Research (CIGEFI) and the School of Physics, University of Costa Rica (UCR). The computational support was supplied by CIGEFI, J.A.A. and D.A.-F. The authors wish to thank Jessy Acuña, Manuel Chaves, Gabriel

Maynard, André Montealegre, Marian Quesada, and Adriana Mora for some data downloading and basic processing. The authors are indebted to the three anonimous reviwers for helpful comments and suggestions to improve the unity and quality of the manuscript. Data comes from the World Wide Lightning Location Network (http://wwlln.net, accessed on 28 December 2021), a collaboration among over 50 universities and institutions, of which the CIGEFI is part of. ERA5 data is available at https://climatedataguide.ucar.edu/climate-data/era5-atmospheric-reanalysis (accessed on 28 December 2021).

Conflicts of Interest: The authors declare no conflict of interest.

References

1. Macleod, M. Mayan calendrics in movement in Guatemala: Mayan spiritual guides or daykeepers understandings of 2012. *J. Lat. Am. Caribb. Anthropol.* **2013**, *18*, 447–464. [CrossRef]
2. Fernández-Torres, S. *Cosmovisión indígena Bribri, Cabécar para docentes indígenas de II Ciclo*, 1st ed.; Freud, S., Psicología de las masas y análisis del yo. Obras completas, Eds.; Departamento de Educación Intercultural. Ministerio de Educación Pública: San José, Costa Rica, 1921; Amorrartu, 2014, 18. (In Spanish)
3. Raga, G.B.; de la Parra, M.G.; Kucienska, B. Deaths by lightning in Mexico (1979–2011): Threat or vulnerability? *Weather. Clim. Soc.* **2014**, *6*, 434–444. [CrossRef]
4. Rohli, R.V.; Li, C. *Meteorology for Coastal Scientists*; Springer Nature: Cham, Switzerland, 2021.
5. Amador, J.A.; Hidalgo, H.G.; Alfaro, E.J.; Calderón, B.; Mora, N. Central America in State of the Climate 2018. *Bull. Am. Meteor. Soc.* **2019**, *100*, S197–S198.
6. Amador, J.A.; Hidalgo, H.G.; Alfaro, E.J.; Calderón, B.; Mora, N. Central America in State of the Climate 2019. *Bull. Am. Meteor. Soc.* **2020**, *101*, S337–S339.
7. Amador, J.A.; Hidalgo, H.G.; Alfaro, E.J.; Calderón, B.; Mora, N. Central America in State of the Climate 2020. *Bull. Am. Meteor. Soc.* **2021**, *102*, S371–S373.
8. Kochtubajda, B.; Stewart, R.E.; Gyakum, J.R.; Flannigan, M.D. Summer convection and lightning over the Mackenzie River Basin and their impacts during 1994 and 1995. *Atmos. Ocean* **2002**, *40*, 199–220. [CrossRef]
9. De La Ree, J.; Liu, Y.; Mili, L.; Phadke, A.G.; Dasilva, L. Catastrophic failures in power systems: Causes, analyses, and countermeasures. *Proc. IEEE* **2005**, *93*, 956–964. [CrossRef]
10. Montana, J.; Morales, C.; Nicora, M.G.; Ardila, J.; Schurch, R.; Aranguren, D. Lightning activity over Chilean territory. *J. Geophys. Res. Atmos.* **2021**, *126*, e2021JD034580. [CrossRef]
11. AlQuran, A.; Batra, M.; Harry Susanto, N.; Holland, A.E.; Davies, J.M.; Erbas, B.; Lampugnani, E.R. Community response to the impact of thunderstorm asthma using smart technology. *Allergy Rhinol.* **2021**, *12*, 21526567211010728. [CrossRef]
12. Muñoz, Á.G.; Díaz-Lobatón, J.; Chourio, X.; Stock, M.J. Seasonal prediction of lightning activity in north western Venezuela: Large-scale versus local drivers. *Atmos. Res.* **2016**, *172*, 147–162. [CrossRef]
13. Montanyà, J.; van der Velde, O.; Williams, E.R. The start of lightning: Evidence of bidirectional lightning initiation. *Sci. Rep.* **2015**, *5*, 1–6. [CrossRef] [PubMed]
14. Sadighi, S. Initiation of Streamers from Thundercloud Hydrometeors and Implication to Lightning Initiation. Ph.D. Thesis, College of Science at Florida Institute of Technology, Melbourne, FL, USA, 2015. Space Principal.
15. Arce-Fernández, D.; Amador, J.A. Actividad eléctrica asociada al huracán Otto (2016) en el Mar Caribe y en el Corredor Seco Centroamericano. *Rev. Bras. De Meteorol.* **2020**, *36*, 1–13. [CrossRef]
16. Collier, A.B.; Bremer, S.; Lichtenberger, J.; Downs, J.R.; Rodger, C.J.; Steinbach, P.; McDowell, G. Global lightning distribution and whistlers observed at Dunedin, New Zealand. *Ann. Geophys.* **2010**, *28*, 499–513. [CrossRef]
17. Nicora, M.; La Fata, A.; Fiori, E.; Delfino, F. Electromagnetic transients on power plant connection caused by lightning event. In Proceedings of the 2021 12th International Symposium on Advanced Topics in Electrical Engineering (ATEE), Bucharest, Romania, 25–27 March 2021; pp. 1–6.
18. Alfita, R.; Ibadillah, A.F.; Nahari, R.V.; Pramudia, M. Analysis of lightning disturbance at 150 kV high voltage power lines. In *Proceedings of the IOP Conference Series: Earth and Environmental Science, Bristol, UK, May 2021*; IOP Publishing: Bristol, UK, 2021; Volume 753, p. 012052.
19. Mansoor, V.M.; Nagaveni, P.; Amudha, A.; Divyapriya, S.; Emayavaramban, G.; Ramkumar, M.S.; SivaramKrishnan, M. Throwing light on lightning. *Mater. Today Proc.* **2021**, *37*, 2572–2577. [CrossRef]
20. Damianaki, K.; Christodoulou, C.A.; Kokalis, C.C.A.; Kyritsis, A.; Ellinas, E.D.; Vita, V.; Gonos, I.F. Lightning protection of photovoltaic systems: Computation of the developed potentials. *Appl. Sci.* **2021**, *11*, 337. [CrossRef]
21. Hunting, E.R.; Matthews, J.; de Arróyabe Hernáez, P.F.; England, S.J.; Kourtidis, K.; Koh, K.; Nicoll, K.; Harrison, R.G.; Manser, K.; Price, C.; et al. Challenges in coupling atmospheric electricity with biological systems. *Int. J. Biometeorol.* **2021**, *65*, 45–58. [CrossRef]
22. Amador, J. A climatic feature of the tropical Americas: The trade wind easterly jet. *Tópicos Meteorológicos Y Oceanográficos* **1998**, *5*, 91–102.

23. Amador, J.A. The intra-Americas seas low-level jet (IALLJ): Overview and future research. *Ann. N. Y. Acad. Sci.* **2008**, *1146*, 153–188. [CrossRef] [PubMed]
24. Poveda, G.; Mesa, O. La corriente de chorro superficial del Oeste ("del Chocó") y otras dos corrientes de chorro en Colombia: Climatología y variabilidad durante las fases del ENSO. *Rev. Académica Colomb. Cienc.* **1999**, *23*, 517–528. (In Spanish)
25. Magaña, V.; Amador, J.A.; Medina, S. The midsummer drought over Mexico and Central America. *J. Clim.* **1999**, *12*, 1577–1588. [CrossRef]
26. Mo, K.C.; Chelliah, M.; Carrera, M.L.; Higgins, R.W.; Ebisuzaki, W. Atmospheric moisture transport over the United States and Mexico as evaluated in the NCEP regional reanalysis. *J. Hydrometeor.* **2005**, *6*, 710–728. [CrossRef]
27. Durán-Quesada, A.; Gimeno, L.; Amador, J.; Nieto, R. A Lagrangian approach to moisture sources for Central America: Part I. Moisture sources identification. *J. Geophys. Res.* **2010**, *115*. [CrossRef]
28. Durán-Quesada, A.M.; Gimeno, L.; Amador, J. Role of moisture transport for Central American precipitation. *Earth Syst. Dyn.* **2017**, *8*, 147–161. [CrossRef]
29. Bürgesser, R.E.; Nicora, M.G.; Avila, E.E. Characterization of the lightning activity of "Relámpago del Catatumbo". *J. Atmos. Sol. Terr. Phys.* **2012**, *77*, 241–247. [CrossRef]
30. Kucienska, B.; Raga, G.B.; Romero Centeno, R. High lightning activity in maritime clouds near Mexico. *Atmos. Chem. Phys.* **2012**, *12*, 8055–8072. [CrossRef]
31. Berry, G.; Reeder, M.J. Objective identification of the intertropical convergence zone: Climatology and trends from the ERA-interim. *J. Clim.* **2014**, *27*, 1894–1909. [CrossRef]
32. Schneider, T.; Bischoff, T.; Haug, G.H. Migrations and dynamics of the intertropical convergence zone. *Nature* **2014**, *513*, 45–53. [CrossRef]
33. Arias, P.A.; Martínez, J.A.; Vieira, S.C. Moisture sources to the 2010–2012 anomalous wet season in northern South America. *Clim. Dyn.* **2015**, *45*, 2861–2884. [CrossRef]
34. Amador, J.A.; Rivera, E.R.; Durán-Quesada, A.M.; Mora, G.; Sáenz, F.; Calderón, B.; Mora, N. The easternmost tropical Pacific. Part I: A climate review. *Rev. Biol. Trop.* **2016**, *64*, S1–S22. [CrossRef]
35. Amador, J.A.; Durán-Quesada, A.M.; Rivera, E.R.; Mora, G.; Sáenz, F.; Calderón, B.; Mora, N. The easternmost tropical Pacific. Part II: Seasonal and intraseasonal modes of atmospheric variability. *Rev. Biol. Trop.* **2016**, *64*, S3–S57. [CrossRef]
36. Wang, C.; Enfield, D.B. The tropical Western Hemisphere warm pool. *Geophys. Res. Lett.* **2001**, *28*, 1635–1638. [CrossRef]
37. Wang, C.; Enfield, D.B. A further study of the tropical Western Hemisphere warm pool. *J. Clim.* **2003**, *16*, 1476–1493. [CrossRef]
38. Schultz, D.M.; Bracken, W.E.; Bosart, L.F. Planetary-and synoptic-scale signatures associated with Central American cold surges. *Mon. Weather. Rev.* **1998**, *126*, 5–27. [CrossRef]
39. Schultz, D.M.; Bracken, W.E.; Bosart, L.F.; Hakim, G.J.; Bedrick, M.A.; Dickinson, M.J.; Tyle, K.R. The 1993 superstorm cold surge: Frontal structure, gap flow, and tropical impact. *Mon. Weather. Rev.* **1997**, *125*, 5–39. [CrossRef]
40. Zárate-Hernández, E. Climatología de masas invernales de aire frío que alcanzan Centroamérica y el Caribe y su relación con algunos índices Árticos. *Tópicos Meteorológicos Y Oceanográficos* **2013**, *12*, 35–55. (In Spanish)
41. Zárate-Hernández, E. Influencia de las masas invernales de aire frío sobre el Chorro de Bajo Nivel del Caribe y sus ramas. *Tópicos Meteorológicos y Oceanográficos* **2014**, *13*, 19–40. (In Spanish)
42. Hidalgo, H.G.; Durán-Quesada, A.M.; Amador, J.A.; Alfaro, E.J. The Caribbean low-level jet, the inter-tropical convergence zone and precipitation patterns in the Intra-Americas Sea: A proposed dynamical mechanism. *Geogr. Ann. Ser. A Phys. Geogr.* **2015**, *97*, 41–59. [CrossRef]
43. Sáenz, F.; Amador, J.A. Características del ciclo diurno de precipitación en el Caribe de Costa Rica. *Rev. Climatol.* **2016**, *6*, 21–34. (In Spanish)
44. Hidalgo, H.G.; Alfaro, E.J.; Amador, J.A.; Bastidas, Á. Precursors of quasi-decadal dry-spells in the Central America Dry Corridor. *Clim. Dyn.* **2019**, *53*, 1307–1322. [CrossRef]
45. Amador, J.A.; Magaña, V.O.; Pérez, J.B. The low level jet and convective activity in the Caribbean. In Proceedings of the 24th Conference on Hurricanes and Tropical Meteorology, Fort Lauderdale, FL, USA, 29 May–2 June 2000; pp. 114–115.
46. Torrealba, E.R.; Amador, J.A. La corriente en chorro de bajo nivel sobre los Llanos Venezolanos de Sur América. *Rev. Climatol.* **2010**, *10*, 1–20.
47. Mora, N.; Amador, J.A.; Rivera, E.R.; Maldonado, T. A Sea Breeze Study during Ticosonde-NAME 2004 in the Central Pacific of Costa Rica: Observations and Numerical Modeling. *Atmosphere* **2020**, *11*, 1333. [CrossRef]
48. Brown, D.P. *Hurricane Otto 20–26 November 2016*; Tropical Cyclone Report; National Hurricane Center: Miami, FL, USA, 2017.
49. Amador, J.A.; Hidalgo, H.G.; Alfaro Durán-Quesada, A.M.; Calderón, B.; Mora, N.; Arce, D. Central America in State of the Climate 2016. *Bull. Amer. Meteor. Soc.* **2017**, *98*, S180–S183. [CrossRef]
50. Stumpf, H.G. Satellite detection of upwelling in the Gulf of Tehuantepec, Mexico. *J. Phys. Oceanogr.* **1975**, *5*, 383–388. [CrossRef]
51. Douglas, M.W.; Fernández, W.; Peña, M. Design and evolution of the PACS SONET observing system in Latin America. In Proceedings of the Third Symposium on Integrated Observing Systems, Dallas, TX, USA, 10–15 June 1999; pp. 10–15.
52. Wyrtki, K. Upwelling in the Costa Rica dome. *Fish. Bull. Fish Wildl. Serv.* **1964**, *63*, 355.
53. Fiedler, P.C. The annual cycle and biological effects of the Costa Rica Dome. *Deep. Sea Res. Part I Oceanogr. Res. Pap.* **2002**, *49*, 321–338. [CrossRef]
54. Kessler, W.S. The circulation of the eastern tropical Pacific: A review. *Prog. Oceanogr.* **2006**, *69*, 181–217. [CrossRef]

55. Virts, K.S.; Wallace, J.M.; Hutchins, M.L.; Holzworth, R.H. Highlights of a new ground-based, hourly global lightning climatology. *Bull. Am. Meteorol. Soc.* **2013**, *94*, 1381–1391. [CrossRef]
56. Lay, E.H.; Rodger, C.J.; Holzworth, R.H.; Dowden, R.L. Introduction to the world wide lightning location network (WWLLN). *Geophys. Res. Abstr.* **2005**, *7*, 02875.
57. Hutchins, M.L.; Holzworth, R.H.; Brundell, J.B.; Rodger, C.J. Relative detection efficiency of the world wide lightning location network. *Radio Sci.* **2013**, *47*, RS6005. [CrossRef]
58. Rodger, C.J.; Werner, S.; Brundell, J.B.; Lay, E.H.; Thomson, N.R.; Holzworth, R.H.; Dowden, R.L. Detection efficiency of the VLF World-Wide Lightning Location Network (WWLLN): Initial case study. In *Annales Geophysicae*; Copernicus GmbH: Göttingen, Germany, 2006; Volume 24, pp. 3197–3214.
59. Lin, S.J.; Chou, K.H. The Lightning Distribution of Tropical Cyclones over the Western North Pacific. *Mon. Weather. Rev.* **2020**, *148*, 4415–4434. [CrossRef]
60. Venugopal, V.; Virts, K.; Sukhatme, J.; Wallace, J.M.; Chattopadhyay, B. A comparison of the fine-scale structure of the diurnal cycle of tropical rain and lightning. *Atmos. Res.* **2016**, *169*, 515–522. [CrossRef]
61. Minobe, S.; Park, J.H.; Virts, K.S. Diurnal cycles of precipitation and lightning in the tropics observed by TRMM3G68, GSMaP, LIS, and WWLLN. *J. Clim.* **2020**, *33*, 4293–4313. [CrossRef]
62. Birch, C.E.; Roberts, M.J.; Garcia-Carreras, L.; Ackerley, D.; Reeder, M.J.; Lock, A.P.; Schiemann, R. Sea-breeze dynamics and convection initiation: The influence of convective parameterization in weather and climate model biases. *J. Clim.* **2015**, *28*, 8093–8108. [CrossRef]
63. Troncoso-Lozada, O. Twelve years of continuous measurements of atmospheric electrical activity in México's Tropical highland. *Atmósfera* **2004**, *17*, 56–67.
64. Albrecht, R.I.; Goodman, S.J.; Buechler, D.E.; Blakeslee, R.J.; Christian, H.J. Where are the lightning hotspots on Earth? *Bull. Am. Meteorol. Soc.* **2016**, *97*, 2051–2068. [CrossRef]
65. Lizano, O.G.; Amador, J.A.; Soto, R. Caracterización de manglares de Centroamérica con sensores remotos. *Rev. Biol. Tro. Int. J. Trop. Biol. Conserv.* **2001**, *48*, 33–51. (In Spanish). Ecosistemas Acuáticos de Costa Rica.
66. Chang, C.H.; Xie, S.P.; Schneider, N.; Qiu, B.; Small, J.; Zhuang, W.; Taguchi, B.; Sasaki, H.; Lin, X. East Pacific ocean eddies and their relationship to subseasonal variability in Central American wind jets. *J. Geophys. Res. Ocean.* **2012**, *117*, C10001. [CrossRef]
67. Maldonado, T.; Rutgersson, A.; Caballero, R.; Pausata, F.S.; Alfaro, E.; Amador, J. The role of the meridional sea surface temperature gradient in controlling the Caribbean low-level jet. *J. Geophys. Res. Atmos.* **2017**, *122*, 5903–5916. [CrossRef]
68. Burpee, R.W. The origin and structure of easterly waves in the lower troposphere of North Africa. *J. Atmos. Sci.* **1972**, *29*, 77–90. [CrossRef]